

An Experimental Approach to Fluctuation of Stress Intensity Factor Distribution and Fatigue Crack Propagation in HSLA Steel

Om Prakash Tenduwe*, Pyare Lal Khunte**, Pawan Kumar Sahu***, Navratan Kumar****

*(Department of Mechanical Engineering, Institute of Technology, Korba, Chhattisgarh, INDIA

** (PG student in Department of Mechanical Engineering, N.I.T. Jamshedpur, Jharkhand, INDIA)

*** (Department of Mechanical Engineering, I.T. G.G.U, Bilaspur, Chhattisgarh, INDIA)

**** (Department of Energy Engineering, Central University, Jharkhand, INDIA)

ABSTRACT

The fluctuation of stress intensity factor distribution and fatigue crack propagation in HSLA steel were investigated, for this purpose fatigue crack growth test were carried out on five mutually similar configured standard ICT specimens with reduced thickness using constant amplitude loading cycles under mode-I, with 0.3 stress ratio and maximum load held 11.8 kN. The fluctuation of stress intensity factor distribution were studied experimentally as a function of crack length, elapsed fatigue life cycle and compliance, along with the behavior of fatigue crack propagation in HSLA steel. The fracture morphology was observed by field emission scanning microscopy. ΔK in starting not increased significantly as increasing crack length, number of cycle and compliance, but after reaching the region-II, it is increasing very significantly and slow fatigue crack propagation behavior were observed by the material.

Keywords- fluctuation of stress intensity factor, fatigue crack propagation, constant amplitude loading, stress ratio, compliance.

I. INTRODUCTION

Fatigue and fracture are a common cause of service failure of engineering parts components and structures. It is presumed that an initial crack (similar to the crack which forms and initiates from voids) exists in the specimen. Of course, this assumption is not far away from reality for many industrial components which experience defects during their manufacturing processes [1].

To study about fatigue failure and its related problem is very important for any kind of machine parts, components and engineering structure these relate to various types of loading condition during their operations, most of engineering machine parts and structures are failed by fatigue and fracture causes problem [2], our aim to understand how materials fail and how crack start and propagate, how we control it and our ability to prevent such failures.

From economical and safety point of view an expensive structure and machine component cannot be replaced from service simply on detecting a fatigue crack during operation. Therefore, reliable valuation of fatigue crack growth and fatigue life prediction are crucial so that the parts/structures can be well-timed serviced or replaced [3].

So for preventing of such type failure, study of fatigue and fatigue causes failure along with the

behavior of material under such condition is very important.

1.1 Fluctuation of stress-intensity factor (ΔK)

In fatigue, the main driving force is fluctuation in the stress-intensity factor in a cycle, that is

$$\Delta K = K_{\max} - K_{\min} \quad (1)$$

The loading variables R , ΔK , and K_{\max} are related in accordance with the following relationships [4]:

$$\Delta K = (1 - R) K_{\max}, \text{ For } R \geq 0 \quad (2)$$

$$\text{Where, } R = \frac{K_{\min}}{K_{\max}},$$

$$\text{And, } \Delta K = K_{\max}, \text{ for } R \leq 0 \quad (3)$$

Where K_{\max} is maximum stress intensity factor, K_{\min} minimum stress intensity factor and R is stress ratio.

While the operational definition of ΔK states that ΔK is dependent on various factors as stress ratio stress intensity factors etc.

Fatigue crack growth threshold, (ΔK_{th}) that the asymptotic value of ΔK at which da/dN approaches zero. For most materials an operational, though arbitrary, definition of ΔK_{th} is given as that ΔK which corresponds to a fatigue crack growth rate of $10^{-9} \leq da/dN \leq 10^{-10}$ m/cycle [4]. The threshold

value is affected by crack length and defined as a function of crack length [5]. The main driving factor or crack extension which is called the crack driving force. This force is associated with the ΔK value.

1.2 Fatigue crack propagation rate

The rate at which crack grows has significantly important in determining the life of a material. The propagation of a crack occurs in a region-II and crack growth depending upon initial crack on shear planes. In crack propagation crack can firstly observed in an engineering sense in stage-II crack growth is well-defined as crack growth on a plane normal to maximum tensile stress. As a crack start to propagate, the size of the crack also begins to grow. As a growing crack in the presence of a constant amplitude cyclic stress intensity. A cyclic plastic zone forms at the crack tip, and the growing crack leaves behind a plastic wake. If the plastic zone is sufficiently small that it is embedded within an elastic singularity zone, the conditions at the crack tip are uniquely defined by the current K value, and the crack growth rate is characterized by K_{min} and K_{max} . It is convenient to express the functional relationship for crack growth in the following form [2].

$$\frac{da}{dN} = f(\Delta K, R) \quad (4)$$

Where, $\frac{da}{dN}$ is crack growth per cycle

The influence of the plastic zone and plastic wake on crack growth is implicit in Equation (4), since the size of the plastic zone depends only on K_{min} and K_{max} . Equation (4) can be integrated to estimate fatigue life.

The numbers of cycles are usually determined according to the available fatigue models, such as the Paris model [6]

$$N = \int_{a_0}^{a_f} \frac{da}{C(\Delta k)^m}$$

The rate at which the crack continues to grow depends upon the fluctuation of stress intensity factor. The rate at which a crack grows can be expressed as mathematically by Paris equation [7].

$$\frac{da}{dN} = C(\Delta K)^m \quad (5)$$

Where C and m are material constants that are determined experimentally. According to equation (5), the fatigue crack growth rate depends only on ΔK ; $\frac{da}{dN}$ is insensitive to the R ratio in region-II.

The fatigue life under cyclic loading consisted of two phases, the crack initiation life followed by a crack growth period until failure. The crack initiation period may cover a large percentage of the fatigue life under high-cycle fatigue. In constant amplitude

loading models, the fatigue crack growth analysis of a component that is subjected to a constant amplitude load is the simplest to perform because no load history has to be considered [2].

II. MATERIAL AND EXPERIMENT DETAILS

2.1 Material

The material was studied in current investigation is HSLA steel, collected from the Rourkela steel plant, Rourkela, Odisha. The chemical composition of the material is provided in Table 1

Table-1. Chemical composition of as-received HSLA steel.

Element	wt.%
C	0.20
Mn	1.27
Si	0.25
P	0.021
S	0.014
Al	0.05
V	0.001
Nb	0.05
Mo	0.01
Fe	Balance

2.2 Metallographic specimen preparation and examination

For metallography examination small piece of material cut out from the as-received material and the sample were well prepared, polished and subsequently etched with freshly prepared 2% Nital solution. Well etched metallography specimens of the material were prepared in Longitudinal and Transverse ($L-T$) directions and examined with the help of an optical microscope (Carl Zeiss Microscopy).

2.3 Tensile Testing

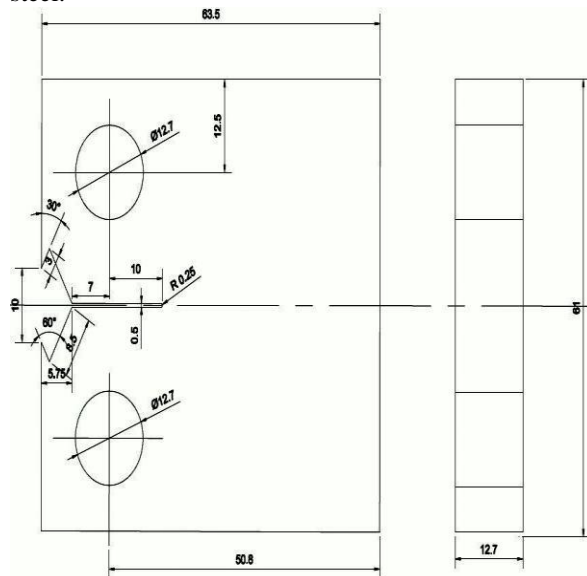
Tensile tests were performed on similarly three round bar specimens of diameter 6 mm and gauge length 30 mm out of the as received material. The tests were conducted following the ASTM standard E8-M [8].

2.4 Fatigue Crack Growth Test

2.4.1 Test specimen geometry

Fatigue crack growth tests, were conducted on 1CT (Compact Tension) specimens with a narrow notch and reduced thickness, which is fabricated from 12.7 mm thick plate. The CT specimens were made in the $L-T$ orientation, both sides of the specimen surfaces were given a mirror-polish with the help of different grades of emery papers with the loading aligned in the longitudinal direction and notch given in the transverse direction, standard ASTM E647-13a [4] are followed for specimen

geometry design. The dimensional details of specimen are presented in Fig. 2.1. Thickness, B, and width, W, of the specimens are equal to 12.7 mm and 50.8 mm, respectively and notch thickness 0.25 mm. The specimens were made from as received HSLA steel.



All dimensions in mm

Fig. 2.1 Compact Tension (CT) specimen geometry (LT orientation) followed by ASTM E 647-13a [4]

2.4.2 Test program

Computer controlled 100 kN load capacity BiSS Universal test machine using VAFCP (Variable amplitude crack propagation) fatigue software. The software permitted on-line monitoring of the crack length (a), compliance, ΔK , load range and the crack growth rate per cycle, (da/dN) . All tests were conducted at the constant amplitude loading mode at stress ratio of (R) 0.3 and using 10 Hz frequency. For fatigue crack growth test performed on CT specimens in accordance with ASTM E647-13a [4].

2.4.3 Fatigue crack growth tests

The specimen surfaces were stick by graph paper to manually examine the crack extension during the test as well as the COD gauge were mounted on the knife edges of specimen to monitor crack extension by the software based program. Fatigue pre-cracking was done under mode-I, loading (crack opening mode) at constant amplitude loading and an a/W ratio of 0.24. All the five tests were done on ambient temperature condition. For determining of the stress intensity factor range (ΔK) for CT specimen were calculated by following equation [4] as:

$$\Delta K = \frac{\Delta P}{B\sqrt{W}} \frac{(2+\alpha)}{(1-\alpha)^{1.5}} (0.886 + 4.64\alpha - 13.32\alpha^2 - 14.72\alpha^3 - 5.6\alpha^4)$$

Where $\alpha = \frac{a}{W}$; expression valid for, $\frac{a}{W} \geq 0.2$.

Table- 2. Test program

Max. load (P_{max}) kN	Mini. Load (P_{min}) kN	Stress Ratio (R)	Initial crack length (a_o) mm	Final crack length (a_f) mm	Frequency (f) Hz
11.8	3.54	0.3	11	34.22	10



Fig. 2.2 (A.) Experimental setup of specimen with COD gauge during test; (B.) Measurement of final crack length by digital Vernier calipers.

2.4.5 Fractography of fatigue fracture surface

Approximately 12 mm long parts of the samples were cut from the fractured surface of fatigue crack growth tested specimen for fractography examinations. The specimen parts were selected as the parts containing as fatigue crack propagated parts of fatigue growth zone. The fractured surfaces were examined with the help of a field emission scanning electron microscopy (FESEM).

III. RESULTS AND DISCUSSIONS

3.1 Microstructural analysis

Well-polished and etched metallography specimens were studied by using an optical microscope. Typical optical micrograph of as-received material is illustrated in Fig.3.1. The white portion of microstructure refers to ferrite and light black portion refers to the pearlite. The dark black portion appears as martensite along with carbide precipitate throughout structure in this steel. The ferrite matrix gives ductility and toughness to the investigated steel.

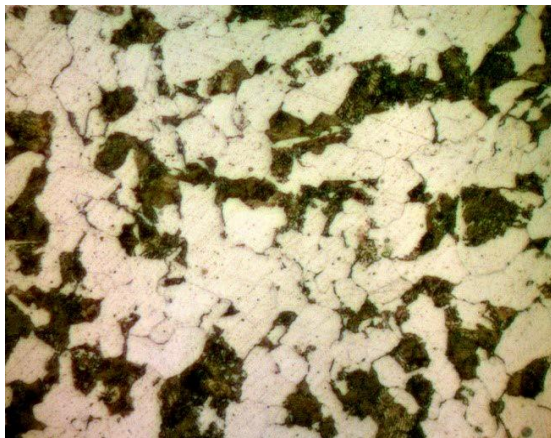


Fig. 3.1 Optical micrograph of as-received material, etched by 2% Nital.

3.2 Tensile properties

The tensile test was carried out on successively three same configured specimen and tensile properties are listed in Table 1. The tensile values are taken by the average of three tests. The 0.2% yield stress and ultimate tensile stress values from the three tests are shown almost same.

Table 3. Mechanical properties of HSLA steel

Yield Strength (σ_{YS}) MPa	622.45
Ultimate Tensile Strength (σ_{UTS}) MPa	778.62
Modulus of Elasticity (E) GPa	210
Poisson ratio (ν)	0.33
% Elongation in 25 mm gauge length	27

3.3 Effect and distribution of fluctuation of stress-intensity factor (ΔK)

Effect and distribution of fluctuation of stress-intensity factor (ΔK) were studied by fatigue crack growth test under constant amplitude load testing on the CT specimen in room temperature condition. The test was done in five mutually same configured CT specimen and that average value are taken for results, it is found that there is approximately same trends and results are found in all the five tests, and the results were shown as a function of elapsed number of cycles, crack length and compliance, it is observed that ΔK increases significantly after reaching mode – II region, before that, in all cases its progress is not much more as compared to the mode-II, ΔK as a function of elapsed cycle is shown on Fig.3.2, from this result it is clear that ΔK increase exponentially with increasing number of the cycle and its increase rapidly when its reaching on mode-II, region. Also from Fig.3.3, when ΔK plotted as a function of crack length, it is found that ΔK increase exponentially

when increasing crack length, but its rate is very fast as compared to number of cycle in mode-I and in the mode-II region its increasing but not as fast as number of cycle case that means the effect of crack length on ΔK is very significant. In case of ΔK distribution with respect to compliance it is shown in Fig. 3.4, that ΔK increase when increasing compliance and trends follows by power law distribution curve. So from above all the results it is found that ΔK distribution is dependent on the above factors and that is affected significantly by ΔK distribution during the test, and it is also noted during test that the fluctuation of stress-intensity factor (ΔK) distribution during a test on the CT specimen is much higher near the notch tip compared to remain area, and crack is started from that area. ΔK in starting not increased significantly as increasing crack length, number of the cycles and compliance, but after reaching the region-II, it was increasing significantly.

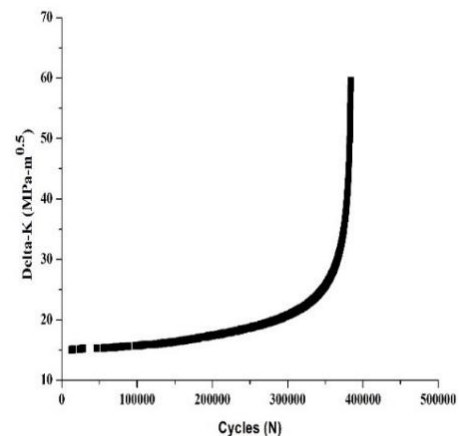


Fig.3.2 Fluctuation of stress-intensity factor (ΔK) versus number of cycles (N) curve.

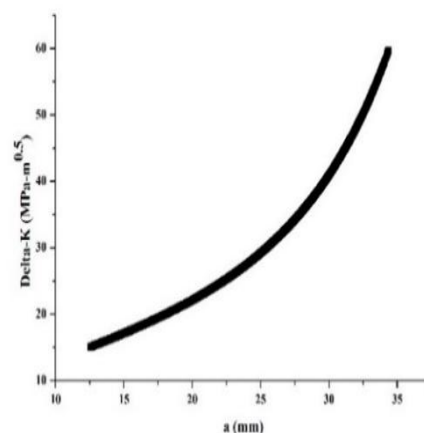


Fig.3.3 Fluctuation of stress-intensity factor (ΔK) versus crack length (a) curve.

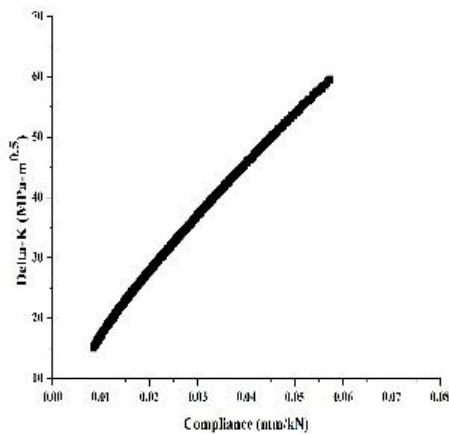


Fig.3.4 Fluctuation of stress-intensity factor (ΔK) versus compliance curve.

3.4 Estimation of threshold cyclic stress intensity factor

The experimental methods for estimating ΔK_{th} are described in the ASTM-E647 standard [4]. In standards, two methods are suggested for estimating ΔK_{th} through da/dN versus ΔK diagram. The first method is K -increasing and the second one is K -decreasing method. The first method holds in the case that $da/dN \geq 10^{-8}$ m/cycles; otherwise, the second method is suitable. In K -increasing method, the value of the stress intensity factor value increases during the test. However, the value of ΔK generally increases during the entire loading. According to ASTM-E647 standard [4], in order to obtain the threshold value of the cyclic stress intensity factor, a line is fitted to the points which are located in the region of $10^{-9} \leq da/dN \leq 10^{-10}$ m/cycle in the fatigue crack growth rate versus cyclic stress intensity factor diagram. Consequently, with regards to the equation of this line, ΔK_{th} is equal to ΔK value corresponding to $10^{-9} \leq da/dN \leq 10^{-10}$ m/cycle. This way, the threshold value of the cyclic stress intensity factor is calculated which is ΔK_{th} equal to $16.33625 \text{ Mpa-m}^{0.5}$

3.5 Fatigue crack propagation in constant amplitude loading

The fatigue crack propagation rate is always increasing with the value of ΔK because a numerically more ΔK represents a greater main driving force to propagate the crack. If the fatigue crack propagates absolutely by a striation-forming mechanism, then da/dN representing the average striation spacing, which gradually increases with the value of ΔK . A typical logarithmic plot of da/dN versus ΔK curve is shown in Fig.3.5 short crack behaviour in fatigue crack growth is generally not well explained by long crack, da/dN versus ΔK

curves, short crack normally starts by growing faster rate than long cracks with similar stress intensity range and then slow down as they get longer cracks. The curve drawn between crack length and number of cycles, from the data obtained from the tests and shown on Fig.3.7 of the steel. It is found that the crack length increases exponentially with respect to number of cycle and from log-log plot of crack growth rates versus stress intensity factors range found that slow fatigue crack propagation were observed, it is due large plastic zone developed near crack tip region during the test so more number of cycles are needed for overcoming this region.

3.6 Calculations of the Paris coefficients

The fatigue crack growth propagation and fatigue lives of the tested specimens were measured under constant amplitude load and stress ratio of 0.3. Also, the Paris coefficients of HSLA steel were calculated using the curve fitting of linear region data of the crack growth rate versus fluctuation of stress intensity factor diagram according to ASTM-E647-13a standard [4]. Fig. 3.5 shows the log-log plot of crack growth rate versus cyclic stress intensity factor diagram for the tested specimens. The linear region follows Paris law ($\frac{da}{dN} = C(\Delta K)^m$). Fitting a line to the linear part of the diagram, the Paris coefficients are obtained as $C = 1 \times 10^{-12}$ and $m = 3.5736$, which are shown in Fig. 3.6.

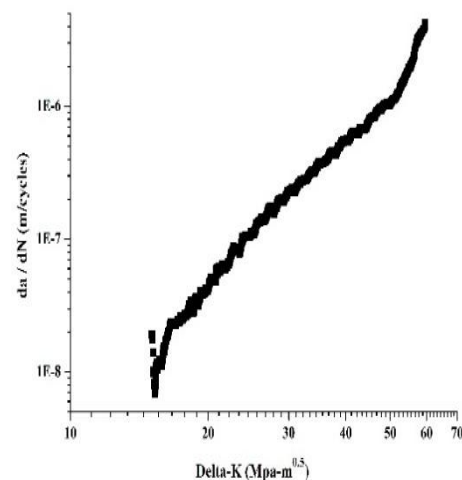


Fig.3.5 log da/dN versus log ΔK curve.

3.7 Fracture surface morphology of fatigue fracture surface

One of the tested specimens were examined under field emission scanning electron microscope (FESEM). FESEM micrograph of constant amplitude loading test at $R=0.3$ are shown in Fig. 3.9. Although the surface indicates the presence of striations.

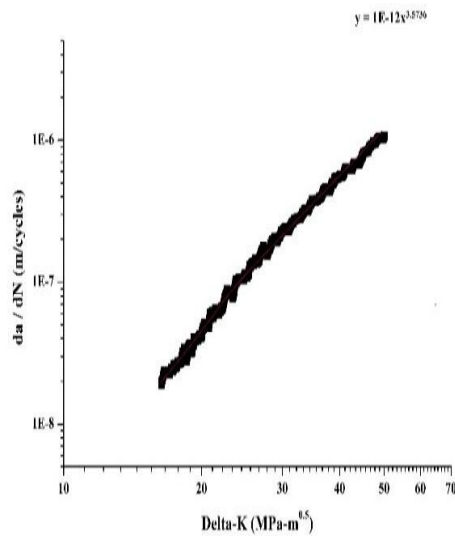


Fig.3.6 log da/dN versus log ΔK curve of linear region.

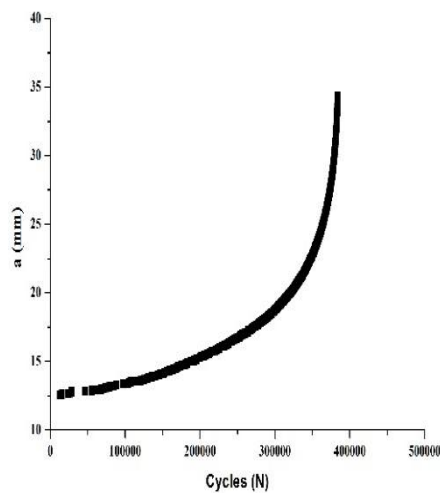


Fig.3.7 Crack length versus number of cycle curve.

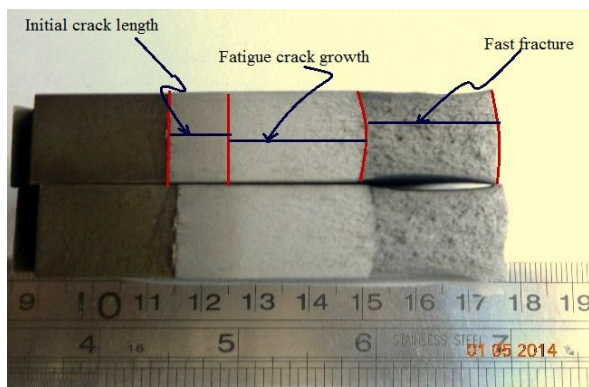


Fig. 3.8 Various region of the fracture surface of fatigue crack growth specimen.

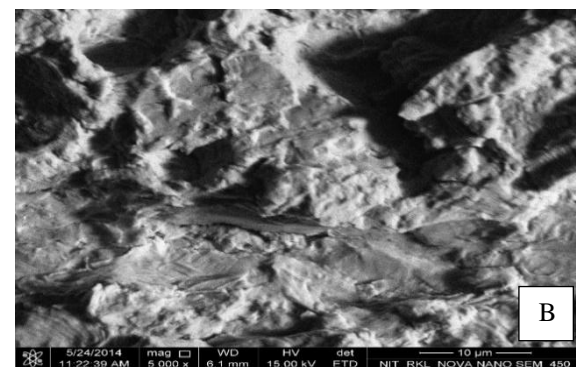
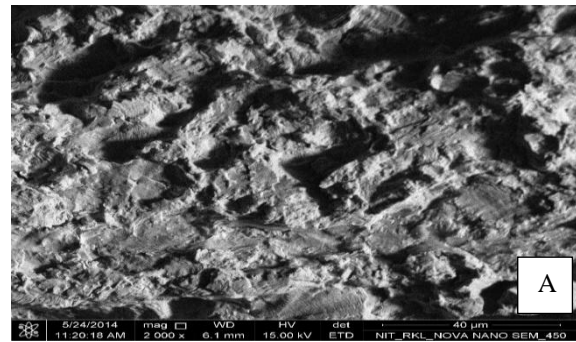


Fig. 3.9 FESEM micrographs of the constant amplitude load fatigue tested, the fracture surface of HSLA steel at stress ratio (R) = 0.3.
 (A.) A microscopic cracks and fine microscopic cracks with stable crack growth.
 (B.) In high magnification showing shallow rough striations in the region of stable crack growth.

IV. CONCLUSION

The following conclusions obtained from the present work are summarized as:

1. The fluctuation of stress intensity factor distribution is strongly dependent on number of cycles, crack length and compliance.
2. The fluctuation of stress intensity factor distribution is increasing more significantly in mode-II compares to mode-I region.
3. The fluctuation of stress intensity factor increasing exponentially when increasing number of cycles and crack length and in case of compliance it is following a power law distribution.
4. The fluctuation of stress intensity factor distribution is very high near crack tip and due to this very large plastic strain field zone formed at the crack tip and for overcoming this effect more number of cycles are needed so resultant fatigue life is increased of this material.
5. The Paris coefficients are obtained as $C = 1 \times 10^{-12}$ and $m = 3.5736$
6. Slow fatigue crack propagation behaviour were observed by the material.

Acknowledgements

The authors are very thankful to Prof. B.B. Verma and Prof. P.K. Ray NIT Rourkela for their kind support, and also wish to thank RSP, SAIL, Rourkela Odisha, INDIA for supplying the materials and we would thanks to Mr. C. Muthuswamy, Dy. General Manager (R&C Lab.) RSP-SAIL for providing chemical analysis of material.

References

- [1] A.R. Shahani, H. Moayeri Kashani, "Assessment of equivalent initial flaw size estimation methods in fatigue life prediction using compact tension specimen tests", *Engineering Fracture Mechanics* 99 (2013) 48–61
- [2] T.L. Anderson, *Fracture Mechanics, fundamentals and Applications*, (CRC Press, Taylor and Francis Group, USA, 2005).
- [3] Om Prakash, *Elastic plastic fracture behavior and effect of band-overload on fatigue crack growth rate of an HSLA Steel*, National Institute of Technology, Rourkela, INDIA, 2014
- [4] ASTM, *Standard Test Method for Measurement of Fatigue Crack Growth Rates*. American Society Testing and Materials, Philadelphia, USA. ASTM E-647-13a. ASTM Standards Handbook.
- [5] Mirco D. Chapetti "Fatigue propagation threshold of short cracks under constant amplitude loading", *International Journal of Fatigue* 25 (2003) 1319–1326
- [6] J.C. Newman, Jr. "The merging of fatigue and fracture mechanics concepts". *Prog. Aerosp. Sci.* 1998; 34:347–90.
- [7] P.C. Paris, and F. Erdogan, "A Critical Analysis of Crack Propagation Laws." *Journal of Basic Engineering*, Vol. 85, 1960, pp. 528–534
- [8] ASTM, *Standard Test Methods for Tension Testing of Metallic Materials*. Annual Book of ASTM Standards, E8/E8M-13a, 2013.